HHS Public Access

Author manuscript

Oncogene. Author manuscript; available in PMC 2016 January 21.

Published in final edited form as:

Oncogene. 2015 July ; 34(27): 3536–3546. doi:10.1038/onc.2014.281.

Kaposi sarcoma-associated herpesvirus promotes tumorigenesis by modulating the Hippo pathway

Guangbo Liu[1,2], **Fa-Xing Yu**[2], **Young Chul Kim**[2], **Zhipeng Meng**[2], **Julian Naipauer**[3], **David J. Looney**[4], **Xiangguo Liu**[1], **J. Silvio Gutkind**[5], **Enrique A. Mesri**[3], and **Kun-Liang Guan**[2]

[1]School of Life Sciences, Shandong University, Jinan 252200, China

[2]Department of Pharmacology and Moores Cancer Center, University of California, San Diego, La Jolla, CA 92130, USA

[3]Miami Center for AIDS Research, Department of Microbiology and Immunology and Viral Oncology Program, Sylvester Comprehensive Cancer Center, University of Miami Miller School of Medicine, Miami, FL 33136, USA

[4]Department of Medicine, VA San Diego Healthcare System, the University of California, San Diego, La Jolla, CA 92093, USA

[5]Oral and Pharyngeal Cancer Branch, National Institute of Dental and Craniofacial Research, National Institutes of Health, Bethesda, MD 20892, USA

Abstract

Kaposi sarcoma-associated herpesvirus (KSHV) is an oncogenic virus and the culprit behind the human disease Kaposi sarcoma (KS), an AIDS-defining malignancy. KSHV encodes a viral G-protein-coupled receptor (vGPCR) critical for the initiation and progression of KS. In this study, we identified that YAP/TAZ, two homologous oncoproteins inhibited by the Hippo tumor suppressor pathway, are activated in KSHV infected cells *in vitro*, KS-like mouse tumors, and clinical human KS specimens. The KSHV-encoded vGPCR acts through Gq/11 and G12/13 to inhibit the Hippo pathway kinases Lats1/2, promoting the activation of YAP/TAZ. Furthermore, depletion of YAP/TAZ blocks vGPCR-induced cell proliferation and tumorigenesis in a xenograft mouse model. The vGPCR-transformed cells are sensitive to pharmacological inhibition of YAP. Our study establishes a pivotal role of the Hippo pathway in mediating the oncogenic activity of KSHV and development of KS, and also suggests a potential of using YAP inhibitors for KS intervention.

Keywords

Kaposi sarcoma; KSHV; vGPCR; Hippo; YAP; TAZ

Corresponding Author: Kun-Liang Guan. RM4010, 2880 Torrey Pines Scenic Dr., La Jolla, CA, 92037-0695, USA, 858-822-7945, kuguan@ucsd.edu.

Conflict of interest

The authors declare that there is no conflict of interest.

Introduction

Kaposi sarcoma (KS) is an AIDS-defining cancer and it is the most frequent type of cancer in males and children living in sub-saharan Africa. KS also affects older patients of Ashkenazy and Mediterranean origin and transplant patients under immunosuppression[1–4]. KS is typically found on the skin, mouth, gastrointestinal tract, and lymph node. Growth rates and size of the tumor vary among patients, and can be life-threatening. Kaposi sarcoma-associated herpesvirus (KSHV, also referred to as HHV-8) has been identified as the infectious agent responsible for KS[3–6]. The incidence of KS in HIV-infected individuals in the United States has been decreasing steadily due to the implementation of antiretroviral therapy[4,7]. However, it retains a high morbidity and mortality in AIDS patients with disseminated disease and some sub-Saharan African countries[6,8,9].

Among the KSHV encoded genes, there is a viral G-protein-coupled receptor (vGPCR) that has been shown to be sufficient to induce neoplastic transformation of endothelial cells and play a necessary non-redundant role in KSHV-induced tumorigenesis[8,10,11]. vGPCR has high basal signaling activity, which can be further enhanced via ligands like CXCL1 (chemokine (C-X-C motif) ligand 1) and CXCL3 (chemokine (C-X-C motif) ligand 3)[12,13]. Mouse models, such as transgenic mice expressing vGPCR and endothelial-specific vGPCR gene transduction (TIE2-tva transgenic mice), have revealed that the vGPCR-induced tumors are remarkably similar to KS[10,14,15], suggesting that vGPCR can drive KS. The precise molecular mechanism whereby vGPCR participates in KSHV-induced oncogenesis is still unclear but it is supposed to involve both direct and paracrine oncogenic effects, which are mediated by growth factors such as VEGF and PDGF induced by vGPCR[4,16].

The Hippo tumor-suppressor pathway is fundamental in regulating organ size, and its dysregulation promotes tumorigenesis[17–22]. Within the Hippo pathway, MST1/2 kinases phosphorylate and activate the Lats1/2 kinases, which in turn phosphorylate and inhibit YAP/TAZ. YAP/TAZ are transcription co-activators with oncogenic potential and their inhibition represents the major functional output of the Hippo pathway. When upstream kinases are repressed, the dephosphorylated YAP/TAZ localize to cell nucleus, associate with TEAD family transcriptional factors (TEAD1-4), and stimulate expression of genes involved in cell survival and proliferation[23–27]. Extensive studies have demonstrated that the Hippo pathway plays important roles in cancer development. For example, transgenic YAP expression in mice induces tissue overgrowth and tumorigenesis[28–30], and deletion of Lats1 results in development of different tumors including sarcoma[31].

Increased YAP/TAZ expression and/or nuclear localization are frequently observed in multiple human cancers[32–36]. However, the mechanisms leading to YAP/TAZ activation in human cancers are largely unknown. In this report, we demonstrate that YAP/TAZ expression is highly elevated in KS, and KSHV-encoded vGPCR signals through the Hippo pathway to induce oncogenic transformation. In addition, downregulation of YAP/TAZ suppresses vGPCR-induced tumorigenesis, and vGPCR-expressing cells are sensitive to pharmacological inhibition of YAP, indicating a pivotal role of the Hippo pathway in the KS development. This work not only reveals a molecular mechanism underlying KS

development upon KSHV infection, but also suggests a potential role of YAP inhibitors for treating KS lesions.

Results

YAP/TAZ expression is elevated in human KS tissues

To determine YAP/TAZ expression in KS, immunohistochemistry (IHC) staining with an antibody that recognizes both YAP and TAZ were performed. The specificity of this antibody for YAP/TAZ in IHC staining was demonstrated by a lack of staining in YAP/TAZ knockdown tissues (Figure S1a). 222 human tissue samples (tissue microarrays obtained from AIDS & Cancer Specimen Resource at University of California, San Francisco) including 26 normal and 196 KS tissues were analyzed. Based on IHC signal intensity, the levels of YAP/TAZ expression were classified into 5 groups (from 0 to 4, with 0 being the weakest and 4 the strongest) (Figure 1a). YAP/TAZ expression in normal tissues was absent or weak. In contrast, most KS tumors showed moderate to high YAP/TAZ expression (Figure 1b). Statistical analysis indicated that YAP/TAZ expression was significantly higher in KS tumors than the normal tissues (Figure 1b). Further analysis of YAP/TAZ expression levels in different KS samples that have more than ten specimens revealed that there was no statistically significant difference of YAP/TAZ expression among KS lesions arising from lymph node, skin, or mouth, indicating that YAP/TAZ activation is a common property in KS independent of tissue origin (Figure 1c). The majority specimens tested are HIV-positive, however all four confirmed HIV-negative specimens exhibited highest YAP/TAZ expression (Figure S1b), suggesting that expression of YAP/TAZ is not associated with HIV infection. Taken together, it appears that YAP/TAZ expression is elevated in KS, and this elevation is independent of tissue origin of KS lesions.

To test if the activation of YAP/TAZ in KS is associated with KSHV infection, we compared the expression of YAP/TAZ and a KSHV-infection marker (latency-associated nuclear antigen, LANA) in clinical KS specimens. IHC staining for LANA was performed in a KS tissue microarray that was a consecutive section to the one used for YAP/TAZ staining. LANA expression levels were also assigned scores ranging from 0 to 4 depending on the staining intensity (Figure S1c). The immune staining signals for YAP/TAZ and LANA were not evenly distributed in the tumor sections. This reflects the nature of KS lesions in which KSHV expression is only spotted in a subset of tumor cells. Interestingly, the distribution of YAP/TAZ signals and LANA signals were remarkably similar (Figure 1d), and the strength of YAP/TAZ signal was positively correlated with LANA expression (R=0.718, Figure 1e). These data suggest that YAP/TAZ are potentially activated by KSHV infection in KS.

Activation of YAP/TAZ by KSHV

YAP/TAZ activity is mainly regulated by Lats1/2, two functionally redundant kinases in the Hippo pathway. Phosphorylation of serine 127 (S127) and additional sites of YAP by Lats1/2 results in YAP cytoplasmic retention, ubiquitination, and degradation[37,38]. TAZ is regulated by Lats1/2 in a similar fashion, although TAZ protein is less stable compared to YAP due to the presence of an additional phosphodegron in TAZ[39,40]. As transcription co-

activators, YAP/TAZ have to be present in the nucleus to induce gene expression. Therefore, the activity of YAP/TAZ can be monitored by their nuclear localization. In addition, YAP/TAZ phosphorylation status and their protein levels (especially for TAZ) are good readouts for their activities. Phosphorylation of YAP can be determined by immunoblotting using a phosphospecific (serine 127, S127) YAP antibody; alternatively YAP phosphorylation can be resolved by Phos-tag gels, in which the slower migrating bands correspond to phosphorylated, hence inactive YAP.

In order to determine if KSHV infection induces YAP/TAZ activation, we examined KS-like mouse allografts with or without KSHV expression. A KSHV-positive cell line (mECK36) was generated by transfection of KSHV bacterial artificial chromosome (KSHVBac36) into mouse bone marrow endothelial lineage cells, and this cell line induced KS-like tumors in mice[11]. In addition, a KSHV-negative tumor was established from explanted mECK36 tumor cells that had lost KSHVBac36 episome. KSHV-negative tumors corresponded to the same cell lineage as mECK36 tumors as verified by transcriptome analysis[41]. The presence or absence of KSHV in both tumors was assessed by IHC staining using a LANA antibody (Figure 2a). We also examined subcellular localization of YAP and/or TAZ in these tumors by IHC using three different antibodies (recognizing YAP, TAZ, or both). Our experiments showed that YAP and/or TAZ were mainly localized in the cytoplasm in KSHV-negative tumors, whereas they were predominantly localized in the nucleus in KSHV-positive tumors (Figure 2a), indicating YAP/TAZ activation only in tumors bearing KSHV.

To further confirm the relationship between KSHV infection and YAP/TAZ activation, we employed an *in vitro* system with either latent or lytic KSHV infection. Human embryonic kidney cells (HEK293A) were latently infected with recombinant KSHV (rKSHV.219) and lytically induction was triggered by sodium butyrate treatment[42]. The expression of lytic KSHV genes upon induction was confirmed using quantitative PCR (Figure 2b, Figure S2a). In this *in vitro* system, we found that the latent infection of KSHV only induced a minor YAP/TAZ activation. On the other hand, following expression of lytic KSHV genes, YAP/TAZ were strongly activated. YAP phosphorylation was dramatically decreased, as revealed by both immunoblotting using a phosphospecific (S127) YAP antibody or Phos-tag gels (Figure 2c). Consistently, TAZ protein level was increased upon lytic induction. Moreover, we observed a significant decrease of Lats1 phosphorylation in its hydrophobic motif (threonine 1079, T1079), which positively correlates with Lats activity, upon induction of lytic KSHV gene expression (Figure 2c), suggesting that Lats1 is inactivated by KSHV. Similar results were observed when HEK293T cells were infected with KSHV (Figure S2b). Taken together, these results suggest that KSHV infection, particularly the lytic KSHV gene expression, leads to Lats inhibition and therefore, activation of YAP/TAZ.

The KSHV-encoded vGPCR activates YAP/TAZ

Among the different lytic KSHV genes, the vGPCR is particularly interesting because it is a major factor contributing to KS pathogenesis[10]. Moreover, GPCR signaling has been shown to regulate the Hippo pathway[43–45]. KS is developed from lymphatic endothelium[2,10,46]. We established a SV40-immortalized murine endothelial cell line (SVEC) stably expressing

HA-tagged vGPCR. Overexpression of vGPCR resulted in YAP dephosphorylation (Phos-tag) and increased YAP protein levels (Figure 3a). The overexpressed vGPCR resolved into multiple bands, which appeared to be due to protein glycosylation (Figure 3a, Figure S3a). vGPCR overexpression also increased TAZ protein levels. The effect of vGPCR on YAP/TAZ activation was further confirmed in additional cell lines, such as HEK293A and the human breast epithelial cells (MCF10A) (Figure 3a). The YAP/TAZ protein elevation in response to vGPCR overexpression was not due to a change in mRNA levels (Figure S2b). However, when protein synthesis was inhibited in the presence of cycloheximide (CHX, an inhibitor for protein synthesis), YAP/TAZ protein stability was increased in vGPCR expressing cells compared to control cells (CHX; Figure 3b, Figure S3c). These results are consistent with previous findings that YAP/TAZ phosphorylation promotes ubiquitination and proteasome-mediated degradation[37,39,47] and demonstrates that vGPCR increases YAP/TAZ protein levels by dephosphorylation and stabilization.

Nuclear localization is required for YAP/TAZ to interact with the transcription factor TEAD and stimulate gene expression. We then assessed the effect of vGPCR expression on YAP/TAZ localization. Cells were cultured in serum-free medium, under which condition YAP/TAZ are cytoplasmic[43]. In control cells, as expected, YAP/TAZ were largely localized in the cytoplasm (Figure 3c). However, YAP/TAZ were enriched in the nucleus in vGPCR expressing cells, consistent with the observed YAP dephosphorylation in vGPCR-expressing cells (Figure 3c, Figure 3a). vGPCR localization was distributed in the plasma membrane and the trans-Golgi network (Figure S3d), which is consistent with previous reports[48,49].

Luciferase reporters driven by a TEAD binding DNA sequence or a fragment of CTGF (connective tissue growth factor, a bona fide YAP/TAZ targeting gene) promoter were used to assess YAP/TAZ activity[23,24,26,27,50,51]. We observed that vGPCR overexpression stimulated activity of both reporters (Figure 3d, Figure S3e). Actually, vGPCR induced stronger reporter activation than the positive control LPAR (LPA receptor), which is known to activate YAP/TAZ[43]. Further supporting a role of vGPCR in YAP/TAZ activation, expression of several known YAP target genes, such as CTGF, CCL2, and SERPINE 1, were also induced by vGPCR expression (Figure 3e). The increased expression of CTGF was also confirmed by Western blotting analysis (Figure 3a). Together, these results reveal that KSHV-encoded vGPCR can induce YAP/TAZ dephosphorylation and nuclear translocation, resulting in transcriptional activation of YAP/TAZ target genes.

vGPCR acts through Gq/11, G12/13, RhoA, and Lats1/2 to stimulate YAP/TAZ

Heterotrimeric G-proteins are required to relay GPCR signals to downstream effectors. To determine the mechanism involved in vGPCR-induced YAP/TAZ expression and activation, we examined the role of Gq/11 and G12/13, which have previously been shown to be important for GPCR-induced activation of YAP/TAZ[43]. Gq/11 or G12/13 are pairs of closely related G alpha proteins with similar functions[52,53], their expression was knocked down by shRNAs. Knockdown of either Gq/11 or G12/13 significantly suppressed YAP/TAZ expression induced by vGPCR (Figure 4a, Figure 4b). Consistently, expression of the YAP/TAZ target gene CTGF was also blocked by knockdown of Gq/11 or G12/13. It is worth noting that knockdown of Gq/11 or G12/13 only partially suppressed YAP/TAZ

activation by vGPCR. This could be due to an incomplete knockdown efficiency, however, another explanation is that Gq/11 and G12/13 act in parallel downstream of vGPCR to activate YAPTAZ.

Previous studies have implicated RhoA GTPase to promote YAP dephosphorylation downstream of G12/13[43,44,54]. Therefore, we investigated RhoA GTPases in vGPCR-induced YAP/TAZ activation. In the presence of dominant negative RhoA (RhoA N19), the effect of vGPCR on TAZ protein levels and CTGF expression was significantly blocked. In contrast, over-expression of constitutively active RhoA (RhoA L63) enhanced TAZ and CTGF protein levels (Figure 4c). Furthermore, expression of Rho-GDI, a Rho GDP-dissociation inhibitor that inhibits Rho, also repressed vGPCR-induced YAP/TAZ activation and CTGF expression (Figure 4d). Based on the above data, we propose that Gq/11, G12/13 and RhoA play an important role in mediating signals from vGPCR to the Hippo pathway.

MST1/2 and Lats1/2 are core components of the Hippo pathway and Lats1/2 directly phosphorylates and inhibits YAP/TAZ[17,28,34]. To determine whether MST1/2 and Lats1/2 are involved in vGPCR induced YAP/TAZ activation, we compared their kinase activity in the absence or presence of vGPCR overexpression. Lats1 was immunoprecipitated (IP) from SVEC control or vGPCR-expressing cells (Figure 4e). Phosphorylation of the hydrophobic motif (T1079) and activation loop (S909) in Lats1 is required for Lats activation[54,55]. In vGPCR overexpressing cells, Lats1 phosphorylation was decreased at both T1079 and S909 sites. Furthermore, in an in vitro kinase assay using bacterially expressed GST-tagged YAP as a substrate, endogenous Lats1 or over-expressed Lats2 immunoprecipitated from vGPCR expressing cells exhibited a weaker kinase activity than Lats1/2 from control cells (Figures 4f, Figure S4a). This data suggests that Lats1/2 is inhibited by vGPCR. Moreover, vGPCR-induced TAZ accumulation and CTGF expression were inhibited when cells were transfected with HA-Lats2 (Figure 4g), further supporting the role of Lats1/2 in vGPCR signaling. Similar experiments were performed with MST1/2 kinases. However, the kinase activity of MST1/2, as judged by the phosphorylation of its substrate Mob, was not significantly changed by vGPCR expression and MST2 overexpression had little effect on vGPCR-induced TAZ accumulation and CTGF expression (Figures 4h, Figure S4b, Figure S4c). These data suggest that vGPCR activates YAP/TAZ by inhibiting Lats1/2 kinases, whereas MST1/2 may not be invovled.

YAP/TAZ mediate vGPCR-induced cell proliferation and migration

Expression of vGPCR promotes cell proliferation and migration. We then tested if the activation of YAP/TAZ contributes to these cellular functions of vGPCR. We established SVEC stable cells expressing vGPCR and shRNAs targeting YAP and/or TAZ. The expression of vGPCR and knockdown of YAP/TAZ in each cell line were confirmed by Western blotting (Figure 5a). We found that knockdown of YAP or TAZ blocked the vGPCR-induced CTGF expression, suggesting that YAP/TAZ mediate biological functions of vGPCR. We also tested the proliferation of the above cell lines under low (0.5%) serum —a condition only supported slow proliferation of control cells. As expected, expression of vGPCR promoted SVEC cell proliferation (Figure 5b). Notably, when YAP or TAZ level

was down-regulated, the vGPCR-enhanced cell proliferation was suppressed. These data demonstrate that vGPCR promotes cell proliferation by activating YAP/TAZ.

To investigate if YAP/TAZ is involved in vGPCR-stimulated cell migration, we utilized both two-dimensional wound healing assay and transwell cell migration assay. In the wound healing assay, expression of vGPCR induced a rapid closure of the wound, whereas when YAP and/or TAZ were depleted, the effect of vGPCR cell migration was largely blocked (Figure 5c). In addition, the transwell migration assay using SVEC or MCF10A cells also showed that the vGPCR-induced cell migration was blocked by depletion of YAP and/or TAZ (Figures 5d, Figure S5). Collectively, our data show that YAP/TAZ play a critical role in vGPCR-induced cell proliferation and migration.

YAP/TAZ are involved in vGPCR-induced tumorigenesis

The above studies have established an important role of YAP/TAZ in vGPCR-induced gene expression and cell proliferation. We next investigated the functional significance of YAP/TAZ in vGPCR-induced tumorigenesis. It has been shown that vGPCR could transform SVEC cells[56]. Thus, we performed soft agar assay to assess anchorage-independent growth of SVEC cells with or without vGPCR expression. Indeed, vGPCR overexpression induced colony formation of SVEC cells in soft agar whereas the control SVEC cells failed to grow. Interestingly, the colony forming ability of the vGPCR-expressing SVEC cells was strongly inhibited when YAP and/or TAZ were depleted (Figure 6a, Figure 6b). Therefore, YAP/TAZ are required for vGPCR to stimulate anchorage-independent growth in SVEC cells.

Next, we examined tumor growth of the above cell lines in a mouse model. Five different cell lines with various manipulations of vGPCR and YAP/TAZ were injected subcutaneously into the immune compromised nude mice. After five weeks, mice were euthanized and tumors were collected. Consistent with the soft agar assay, vGPCR expression induced tumor formation. Importantly, knockdown of YAP/TAZ individually or combinatory impaired the ability of vGPCR to induce tumor formation (Figures 6c, Figure 6d, Figure S6). These results strongly support a critical role of YAP/TAZ in vGPCR-induced tumorigenesis.

vGPCR-expressing cells are sensitive to a YAP inhibitor

To complement the YAP/TAZ knockdown experiments described in Figure 6, we investigated the effect of Verteporfin, a pharmacological YAP inhibitor[50], on cell survival and anchorage-independent growth of SVEC cells expressing vGPCR. We have recently shown that tumorigenesis of active BRAF mutant (V600E) in uveal melanomas is YAP-independent[57]. We have therefore established a SVEC cell line expressing $BRAF^{V600E}$ as a control. Although expression of either vGPCR or $BRAF^{V600E}$ induced ERK phosphorylation, $BRAF^{V600E}$ failed to induce YAP dephosphorylation and TAZ accumulation (Figure 7a). When both cell lines were treated with Verteporfin, the vGPCR-expressing cells were effectively killed, whereas $BRAF^{V600E}$-expressing cells were more resistant to Verteporfin treatment (Figure 7b). When cells were cultured in soft-agar, both cell lines formed colonies, indicating successful transformation by vGPCR or $BRAF^{V600E}$;

however, the anchorage-independent growth of vGPCR-expressing cells, but not $BRAF^{V600E}$-expressing cells, were effectively blocked when cells were treated with Verteporfin (Figure 7c, Figure 7d). These results demonstrate that vGPCR-induced oncogenic transformation is sensitive to YAP inhibition by Verteporfin.

Discussion

In this study, we show that YAP/TAZ activation by vGPCR is pivotal for its transforming and tumorigenic activity. Moreover, we found that YAP/TAZ are activated in KSHV-infected cells of clinical KS specimens, KSHV infected cells, and KS-like mouse tumors. Mechanistically, vGPCR activates YAP/TAZ through Gq/11 or G12/13 and RhoA by inhibiting the Hippo pathway kinases Lats1/2. Our study therefore suggests a pathogenic role of the Hippo pathway in KSHV-induced oncogenesis.

The Hippo pathway is regulated by many upstream signals, such as cell geometry, cell contact, and GPCR signaling[20]. This study provides the first example of the Hippo pathway regulation by virus and establishes a critical role of the Hippo pathway in vGPCR-induced tumorigenesis. Besides KS, KSHV can also cause other types of cancers such as multi centric Castleman's disease and primary effusion lymphoma[58,59]. In addition, other viruses, such as Epstein-Barr virus (HHV-4) and cytomegalovirus (CMV), also contain open reading frames encoding active GPCR[13,60]. We speculate that activation of YAP/TAZ may also contribute to tumorigenesis of multiple cancers induced by virus encoding GPCRs.

YAP/TAZ are frequently elevated in many types of human cancers, however, the underlying mechanism leading to YAP/TAZ activation is largely unknown[32–36,61,62]. This study reveals that a pathogenic virus can activate YAP/TAZ to induce cancer. The involvement of vGPCR in YAP/TAZ activation suggests that in KS, and potentially other types of cancers, YAP/TAZ activation may be a result of dysregulated GPCR signaling, such as by vGPCRs that are ligand independent and constitutively active. In support, it has been recently shown that activation of YAP by *GNAQ* or *GNA11* mutation is indispensible for the development of uveal melanoma, the most common malignancy in adult eyes[57,63]. Therefore, YAP/TAZ may play a broad role in tumorigenesis associated with altered GPCR signaling.

Cancer initiation and development is a complex process requiring alterations of multiple cellular signaling mechanisms. Since vGPCR is an early lytic gene expressed in a minority of KSHV-infected cells of the KS lesions[4,16], our results suggest a direct vGPCR-YAP/TAZ signaling in lytically infected cells, and possibly a paracrine signaling by which vGPCR-induced factors may function as upstream activators for YAP/TAZ in KS lesions. In addition to the Hippo pathway, other signaling pathways have also been implicated in mediating the oncogenic effect of vGPCR[13,64]. For example, PI3Kγ is activated by vGPCR and has an important role in vGPCR-induced sarcomas[65], while NFkB plays a role in vGPCR-induced paracrine neoplasia[66]. It is likely that the activation of YAP/TAZ along with other vGPCR downstream signaling events, such as PI3K and NFkB, collectively contributes to KS tumorigenesis in KSHV infected patients. It is worth noting that YAP/TAZ also induce expression of many growth factors, such as CTGF and insulin-like growth factor (IGF) [23,67], which may therefore contribute to neoplasia induced by vGPCR in a paracrine manner[4,16].

KS remains a serious clinical complication and causes high morbidity and mortality. Mechanistic understanding of KSHV in KS tumorigenesis will provide value for future therapeutic intervention. Our findings demonstrate an essential role of YAP/TAZ activation in mediating KSHV induced tumorigenesis, and also suggest a potential for treating KS lesions using YAP inhibitors.

Materials and methods

Chemicals

The following chemicals were used in this study: C3 (Cytoskeleton Inc), Puromycin (Invivogen), Hygromycin (Invitrogen), Protein Deglycosylation Mix (New England BioLabs), and PolyJet DNA in vitro transfection reagent (SignaGen Laboratories).

Cell culture, transfection, and infection

HEK293A and SVEC cells were cultured in Dulbecco's Modified Eagle Medium (DMEM). MCF10A cells were cultured in DMEM/F12 supplemented with 5% horse serum, 20 ng/mL EGF, 0.5 mg/mL hydrocortisone, 10 mg/mL insulin, and 100 ng/mL cholera toxin. Cells were cultured at 37°C with 5% CO2. Dr. J. Silvio Gutkind (National Institute of Dental and Craniofacial Research, National Institutes of Health) generously provided the SVEC cells.

Cells were transfected using PolyJet DNA in vitro transfection reagent (SignaGen Laboratories), according to the manufacturer's instructions. The pCMV-HA-YAP, pCDNA3-Flag-MST2, and pCDNA3-Flag-Lats2 plasmids have been previously described [37,54]. Rac, Rac-N17, and Rho-GDI were cloned into a pCDNA3 vector. vGPCR was cloned into a pQCXIH retroviral vector. The YAP and TAZ shRNAs targeting human and mouse mRNA were purchased from Sigma and used to make retrovirus to create stable cell lines.

For infection studies, adherent HEK293 cells were infected with rKSHV.219 under puromycin selection as described previously[42,68]. For lytic induction, rKSHV.219-infected HEK293 cells were treated at 70% confluence with 3mM sodium butyrate. Lytic induction was assessed by eGFP and RFP cytofluorometry and by qRT-PCR for KSHV lytic genes as described previously[68]. For tumorigenicity studies in KSHV-positive and negative cells, mECK36, a murine endothelial cell line stably transfected with a KSHV-containing bacterial artificial chromosome (BAC36), is maintained in media further supplemented with 30% FBS, MEM vitamins, insulin, transferrin, selenite, endothelial cell growth supplement, endothelial cell growth factor, and heparin[11]. KSHV-negative mECK36 were obtained from mECK36 tumor explants after Bac36 episome loss achieved by growth without hygromycin selection as previously described [42]. KSHV-negative cells were further selected by weeding and cell sorting. Absence of KSHV genome was verified by PCR for LANA, K1, vIRF-1, ORF23, ORF 36, ORF 74, and K15. KSHV-negative mECK36 cell lineage of cells and tumors was verified by gene microarray[42].

RNA isolation, reverse transcription, and real-time PCR

Cells were washed with cold phosphate-buffered saline (PBS) and RNA was extracted using an RNeasyPlusMinikit (Qiagen). Isolated RNA was quantified and reverse-transcribed using iScript reverse transcriptase (Bio-Rad). cDNA was diluted and quantified by real-time PCR using KAPA SYBR FAST quantitative PCR master mix (KapaBiosystems) and the 7300 real-time PCR system (Applied Biosystems). Primers used in this study were:

YAP-F: CCTTCTTCAAGCCGCCGGAG

YAP-R: CAGTGTCCCAGGAGAAACAGC

TAZ-F: GGCTGGGAGATGACCTTCAC

TAZ-R: AGGCACTGGTGTGGAACTGAC

CTGF-F: CCAATGACAACGCCTCCTG

CTGF-R: TGGTGCAGCCAGAAAGCTC

CCL2-F: ATAGCAGCCACCTTCATTCC

CCL2-R: CTTGCTGCTGGTGATTCTTCT

SERPINE1-F: CTTCATGCCCCACTTCTTCAGG

SERPINE1-R: CACGGCTCCTTTCCCAAGCAA

GAPDH-F: GAAGGTGAAGGTCGGAGT

GAPDH-R: GAAGATGGTGATGGGATTTC

YAP (M)-F: ACCCTCGTTTTGCCATGAAC

YAP (M)-R: TGTGCTGGGATTGATATTCCGTA

TAZ (M)-F: GTCACCAACAGTAGCTCAGATC

TAZ (M)-R: AGTGATTACAGCCAGGTT AGAAAG

β-actin (M)-F: AGCCTTCCTTCTTGGGTATGG

β-actin (R)-R: CACTTGCGGTGCACGATGGAG

Immunoprecipitation and kinase assay

Cells were lysed with mild lysis buffer (50 mM HEPES at pH 7.5, 150 mM NaCl, 1 mM EDTA, 1% NP-40, 10 mM pyrophosphate, 10 mM glycerophosphate, 50 mM NaF, 1.5 mM Na3VO4, protease inhibitor cocktail (Roche), 1 mM PMSF). The protein fraction was obtained by centrifugation and incubated with the appropriate antibodies for 1 hour at 4°C. Protein A or protein G-conjugated beads were added to the protein fraction and incubated for 1 hour. The beads were washed four times in mild lysis buffer. For immunoprecipitation, proteins were eluted by adding SDS-PAGE sample buffer. For the kinase assay, beads were washed once using wash buffer (40 mM HEPES, 200 mM NaCl) and once using the kinase assay buffer (30 mM HEPES, 50 mM potassiumacetate, 5 mM $MgCl_2$). GST-YAP or GST-Mob (expressed and purified from Escherichia coli) was added as the substrate and

incubated for 30 minutes at 30°C. The reaction was terminated by addition of SDS-PAGE sample buffer.

Immunoblotting

Immnuoblotting was performed using a standard protocol. Antibodies for YAP, TAZ (V386), YAP/TAZ, MST1, Lats1, phospho-Lats1/2 (S909/872), and phospho-Lats1/2 (T1079/999) are from Cell Signaling Technology. The HA antibody is from Covance. CTGF, Gq, G11, G12, G13, Myc-HRP, and GFP antibodies are from Santa Cruz Biotechnology. Vinculin, HSP90, and Flag-HRP antibodies were purchased from Sigma-Aldrich.

Luciferase assay

HEK293A cells were seeded onto 24-well plates. The luciferase reporter, Renilla, and the indicated plasmids were co-transfected. Luciferase activity was assayed 24 hours after transfection using the Dual-Luciferase Reporter assay system from Promega following the manufacturer's instructions.

Immunofluorescence staining

The indicated cells were cultured on cover slips. After 24 hours, cells were fixed with 4% paraformaldehyde and permeabilized with 0.1% Triton X-100. Cells were then blocked using 3% BSA for 30 minutes and incubated with the appropriate primary antibody for 1.5 hours at room temperature. Following three washes in PBS, slides were incubated with Alexa Fluor 488- or 546-conjugated secondary antibodies (1:1000 dilutions) from Life Technologies for 1.5 hours. The slides were then washed with PBS and mounted with DAPI.

Cell migration assay

The filter of the chamber was pre-incubated with 20 μg/mL fibronectin for 1 hour. Cells were serum-starved for 24 hours and then seeded into the upper chamber of the insert (BD Falcon cell culture inserts for 24-well plates with 8.0-mm pores) in serum-free medium. The lower chamber was filled with media containing 20% mTeSR1. After 24 hours, cells were fixed using 4% paraformaldehyde and stained using 0.05% crystal violet. Cells in the upper chamber were carefully removed. Cells that migrated through the filter were assessed by photography.

Tumorigenicity in nude mice

Nude mice were subcutaneously injected with 1 X 10^6 SVEC cells, KSHV-positive or KSHV-negative mECK36 cells[42]. Five weeks after injection, mice were euthanized and their tumors were harvested and weighted.

Soft agar colony formation assay

Cells (3 X 10^4) were suspended in complete medium containing 0.4% Nobel agar (Difco) (containing 2 μg/mL puromycin, 300 μg/mL hygromycin) and seeded onto 6-well plates over a basal layer of complete medium containing 0.8% agar. Colonies were stained with crystal violet after 20 days.

Wound healing assay

Cells were seeded onto 6-well plates and grown until fully confluent. The cells were then serum-starved for 24 hours and scraped with a 200 μL tip. After 16 hours, the cells were photographed.

Clinical tissue microarrays analysis

Immunohistochemistry of clinical tissue microarrays was performed using a standard protocol according to VECTOR Laboratories. Antibody staining of YAP/TAZ (Cell Signaling Technology) was diluted to 1:100. The secondary antibody and the DAB peroxidase substrate were purchased from VECTOR Laboratories. The expression of YAP/TAZ was classified into 5 levels depending on the signal strength.

Supplementary Material

Refer to Web version on PubMed Central for supplementary material.

Acknowledgments

We would like to thank AIDS & Cancer Specimen Resource at University of California, San Francisco (particularly Ronald Honrada, Andrew Ma, and Michael McGrath) for providing the tissue microarrays and carrying out the HHV-8 staining. We thank Jenna Jewell, Steve Plouffe, and Fabian Flores for critical reading of this manuscript. Also, we would like to thank Drs. Dirk Dittmer, Carsten Gram Hansen, and Toshiro Moroishi for insightful discussions. EAM and JN would like to thank Santas Rosario and Darlah Lopez Rodriguez for their help with the infection systems. This study was supported by grants from NIH and CIRM to K.L.G and the Chinese Scholarship Council to G.L. E.A.M and J.N. were supported by NIH grants CA136387 and Miami CFAR grant P30AI073961.

References

1. Wen KW, Damania B. Kaposi sarcoma-associated herpesvirus (KSHV): molecular biology and oncogenesis. Cancer Lett. 2010; 289(2):140–150. [PubMed: 19651473]
2. Flore O, Rafii S, Ely S, O'Leary JJ, Hyjek EM, Cesarman E. Transformation of primary human endothelial cells by Kaposi's sarcoma-associated herpesvirus. Nature. 1998; 394(6693):588–592. [PubMed: 9707121]
3. Hermans P. Kaposi's sarcoma in HIV-infected patients: treatment options. HIV Med. 2000; 1(3): 137–142. [PubMed: 11737340]
4. Mesri EA, Cesarman E, Boshoff C. Kaposi's sarcoma and its associated herpesvirus. Nat Rev Cancer. 2010; 10(10):707–719. [PubMed: 20865011]
5. Ganem D. KSHV infection and the pathogenesis of Kaposi's sarcoma. Annu Rev Pathol. 2006; 1:273–296. [PubMed: 18039116]
6. Chang Y, Cesarman E, Pessin MS, Lee F, Culpepper J, Knowles DM, et al. Identification of herpesvirus-like DNA sequences in AIDS-associated Kaposi's sarcoma. Science. 1994; 266(5192): 1865–1869. [PubMed: 7997879]
7. Ledergerber B, Egger M, Erard V, Weber R, Hirschel B, Furrer H, et al. AIDS-related opportunistic illnesses occurring after initiation of potent antiretroviral therapy: the Swiss HIV Cohort Study. JAMA. 1999; 282(23):2220–2226. [PubMed: 10605973]
8. Ganem D. KSHV and the pathogenesis of Kaposi sarcoma: listening to human biology and medicine. J Clin Invest. 2010; 120(4):939–949. [PubMed: 20364091]
9. Edelman DC. Human herpesvirus 8--a novel human pathogen. Virol J. 2005; 2:78. [PubMed: 16138925]
10. Montaner S, Sodhi A, Molinolo A, Bugge TH, Sawai ET, He Y, et al. Endothelial infection with KSHV genes in vivo reveals that vGPCR initiates Kaposi's sarcomagenesis and can promote the tumorigenic potential of viral latent genes. Cancer Cell. 2003; 3(1):23–36. [PubMed: 12559173]

11. Mutlu AD, Cavallin LE, Vincent L, Chiozzini C, Eroles P, Duran EM, et al. In vivo-restricted and reversible malignancy induced by human herpesvirus-8 KSHV: a cell and animal model of virally induced Kaposi's sarcoma. Cancer Cell. 2007; 11(3):245–258. [PubMed: 17349582]
12. Gershengorn MC, Geras-Raaka E, Varma A, Clark-Lewis I. Chemokines activate Kaposi's sarcoma-associated herpesvirus G protein-coupled receptor in mammalian cells in culture. J Clin Invest. 1998; 102(8):1469–1472. [PubMed: 9788958]
13. Montaner S, Kufareva I, Abagyan R, Gutkind JS. Molecular mechanisms deployed by virally encoded G protein-coupled receptors in human diseases. Annu Rev Pharmacol Toxicol. 2013; 53:331–354. [PubMed: 23092247]
14. Guo HG, Sadowska M, Reid W, Tschachler E, Hayward G, Reitz M. Kaposi's sarcoma-like tumors in a human herpesvirus 8 ORF74 transgenic mouse. J Virol. 2003; 77(4):2631–2639. [PubMed: 12552002]
15. Yang TY, Chen SC, Leach MW, Manfra D, Homey B, Wiekowski M, et al. Transgenic expression of the chemokine receptor encoded by human herpesvirus 8 induces an angioproliferative disease resembling Kaposi's sarcoma. J Exp Med. 2000; 191(3):445–454. [PubMed: 10662790]
16. Cavallin LE, Goldschmidt-Clermont P, Mesri EA. Molecular and Cellular Mechanisms of KSHV Oncogenesis of Kaposi's Sarcoma Associated with HIV/AIDS. PLoS Pathog. 2014; 10(7):e1004154. [PubMed: 25010730]
17. Pan D. Hippo signaling in organ size control. Genes Dev. 2007; 21(8):886–897. [PubMed: 17437995]
18. Zhao B, Li L, Lei Q, Guan KL. The Hippo-YAP pathway in organ size control and tumorigenesis: an updated version. Genes Dev. 2010; 24(9):862–874. [PubMed: 20439427]
19. Harvey KF, Zhang X, Thomas DM. The Hippo pathway and human cancer. Nat Rev Cancer. 2013; 13(4):246–257. [PubMed: 23467301]
20. Yu FX, Guan KL. The Hippo pathway: regulators and regulations. Genes Dev. 2013; 27(4):355–371. [PubMed: 23431053]
21. Pan D. The hippo signaling pathway in development and cancer. Dev Cell. 2010; 19(4):491–505. [PubMed: 20951342]
22. Johnson R, Halder G. The two faces of Hippo: targeting the Hippo pathway for regenerative medicine and cancer treatment. Nat Rev Drug Discov. 2013
23. Zhao B, Ye X, Yu J, Li L, Li W, Li S, et al. TEAD mediates YAP-dependent gene induction and growth control. Genes Dev. 2008; 22(14):1962–1971. [PubMed: 18579750]
24. Zhang L, Ren F, Zhang Q, Chen Y, Wang B, Jiang J. The TEAD/TEF family of transcription factor Scalloped mediates Hippo signaling in organ size control. Dev Cell. 2008; 14(3):377–387. [PubMed: 18258485]
25. Goulev Y, Fauny JD, Gonzalez-Marti B, Flagiello D, Silber J, Zider A. SCALLOPED interacts with YORKIE, the nuclear effector of the hippo tumor-suppressor pathway in Drosophila. Curr Biol. 2008; 18(6):435–441. [PubMed: 18313299]
26. Vassilev A, Kaneko KJ, Shu H, Zhao Y, DePamphilis ML. TEAD/TEF transcription factors utilize the activation domain of YAP65, a Src/Yes-associated protein localized in the cytoplasm. Genes Dev. 2001; 15(10):1229–1241. [PubMed: 11358867]
27. Wu S, Liu Y, Zheng Y, Dong J, Pan D. The TEAD/TEF family protein Scalloped mediates transcriptional output of the Hippo growth-regulatory pathway. Dev Cell. 2008; 14(3):388–398. [PubMed: 18258486]
28. Dong J, Feldmann G, Huang J, Wu S, Zhang N, Comerford SA, et al. Elucidation of a universal size-control mechanism in Drosophila and mammals. Cell. 2007; 130(6):1120–1133. [PubMed: 17889654]
29. Camargo FD, Gokhale S, Johnnidis JB, Fu D, Bell GW, Jaenisch R, et al. YAP1 increases organ size and expands undifferentiated progenitor cells. Curr Biol. 2007; 17(23):2054–2060. [PubMed: 17980593]
30. von Gise A, Lin Z, Schlegelmilch K, Honor LB, Pan GM, Buck JN, et al. YAP1, the nuclear target of Hippo signaling, stimulates heart growth through cardiomyocyte proliferation but not hypertrophy. Proc Natl Acad Sci U S A. 2012; 109(7):2394–2399. [PubMed: 22308401]

31. St JM, Tao W, Fei X, Fukumoto R, Carcangiu ML, Brownstein DG, et al. Mice deficient of Lats1 develop soft-tissue sarcomas, ovarian tumours and pituitary dysfunction. Nat Genet. 1999; 21(2): 182–186. [PubMed: 9988269]
32. Chan SW, Lim CJ, Guo K, Ng CP, Lee I, Hunziker W, et al. A role for TAZ in migration, invasion, and tumorigenesis of breast cancer cells. Cancer Res. 2008; 68(8):2592–2598. [PubMed: 18413727]
33. Steinhardt AA, Gayyed MF, Klein AP, Dong J, Maitra A, Pan D, et al. Expression of Yes-associated protein in common solid tumors. Hum Pathol. 2008; 39(11):1582–1589. [PubMed: 18703216]
34. Zhao B, Wei X, Li W, Udan RS, Yang Q, Kim J, et al. Inactivation of YAP oncoprotein by the Hippo pathway is involved in cell contact inhibition and tissue growth control. Genes Dev. 2007; 21(21):2747–2761. [PubMed: 17974916]
35. Fernandez-L A, Northcott PA, Dalton J, Fraga C, Ellison D, Angers S, et al. YAP1 is amplified and up-regulated in hedgehog-associated medulloblastomas and mediates Sonic hedgehog-driven neural precursor proliferation. Genes Dev. 2009; 23(23):2729–2741. [PubMed: 19952108]
36. Xu MZ, Yao TJ, Lee NP, Ng IO, Chan YT, Zender L, et al. Yes-associated protein is an independent prognostic marker in hepatocellular carcinoma. Cancer. 2009; 115(19):4576–4585. [PubMed: 19551889]
37. Zhao B, Li L, Tumaneng K, Wang CY, Guan KL. A coordinated phosphorylation by Lats and CK1 regulates YAP stability through SCF(beta-TRCP). Genes Dev. 2010; 24(1):72–85. [PubMed: 20048001]
38. Hao Y, Chun A, Cheung K, Rashidi B, Yang X. Tumor suppressor LATS1 is a negative regulator of oncogene YAP. J Biol Chem. 2008; 283(9):5496–5509. [PubMed: 18158288]
39. Liu CY, Zha ZY, Zhou X, Zhang H, Huang W, Zhao D, et al. The hippo tumor pathway promotes TAZ degradation by phosphorylating a phosphodegron and recruiting the SCF{beta}-TrCP E3 ligase. J Biol Chem. 2010; 285(48):37159–37169. [PubMed: 20858893]
40. Lei QY, Zhang H, Zhao B, Zha ZY, Bai F, Pei XH, et al. TAZ promotes cell proliferation and epithelial-mesenchymal transition and is inhibited by the hippo pathway. Mol Cell Biol. 2008; 28(7):2426–2436. [PubMed: 18227151]
41. Ma Q, Cavallin LE, Leung HJ, Chiozzini C, Goldschmidt-Clermont PJ, Mesri EA. A role for virally induced reactive oxygen species in Kaposi's sarcoma herpesvirus tumorigenesis. Antioxid Redox Signal. 2013; 18(1):80–90. [PubMed: 22746102]
42. Vieira J, O'Hearn PM. Use of the red fluorescent protein as a marker of Kaposi's sarcoma-associated herpesvirus lytic gene expression. Virology. 2004; 325(2):225–240. [PubMed: 15246263]
43. Yu FX, Zhao B, Panupinthu N, Jewell JL, Lian I, Wang LH, et al. Regulation of the Hippo-YAP pathway by G-protein-coupled receptor signaling. Cell. 2012; 150(4):780–791. [PubMed: 22863277]
44. Mo JS, Yu FX, Gong R, Brown JH, Guan KL. Regulation of the Hippo-YAP pathway by protease-activated receptors (PARs). Genes Dev. 2012; 26(19):2138–2143. [PubMed: 22972936]
45. Yu FX, Zhang Y, Park HW, Jewell JL, Chen Q, Deng Y, et al. Protein kinase A activates the Hippo pathway to modulate cell proliferation and differentiation. Genes Dev. 2013; 27(11):1223–1232. [PubMed: 23752589]
46. Kahn HJ, Bailey D, Marks A. Monoclonal antibody D2-40, a new marker of lymphatic endothelium, reacts with Kaposi's sarcoma and a subset of angiosarcomas. Mod Pathol. 2002; 15(4):434–440. [PubMed: 11950918]
47. Tian Y, Kolb R, Hong JH, Carroll J, Li D, You J, et al. TAZ promotes PC2 degradation through a SCFbeta-Trcp E3 ligase complex. Mol Cell Biol. 2007; 27(18):6383–6395. [PubMed: 17636028]
48. Feng H, Dong X, Negaard A, Feng P. Kaposi's sarcoma-associated herpesvirus K7 induces viral G protein-coupled receptor degradation and reduces its tumorigenicity. PLoS Pathog. 2008; 4(9):e1000157. [PubMed: 18802460]
49. Chiou CJ, Poole LJ, Kim PS, Ciufo DM, Cannon JS, Ap RC, et al. Patterns of gene expression and a transactivation function exhibited by the vGCR (ORF74) chemokine receptor protein of Kaposi's sarcoma-associated herpesvirus. J Virol. 2002; 76(7):3421–3439. [PubMed: 11884567]

50. Liu-Chittenden Y, Huang B, Shim JS, Chen Q, Lee SJ, Anders RA, et al. Genetic and pharmacological disruption of the TEAD-YAP complex suppresses the oncogenic activity of YAP. Genes Dev. 2012; 26(12):1300–1305. [PubMed: 22677547]
51. Chan SW, Lim CJ, Chong YF, Pobbati AV, Huang C, Hong W. Hippo pathway-independent restriction of TAZ and YAP by angiomotin. J Biol Chem. 2011; 286(9):7018–7026. [PubMed: 21224387]
52. Ibarrondo J, Joubert D, Dufour MN, Cohen-Solal A, Homburger V, Jard S, et al. Close association of the alpha subunits of Gq and G11 G proteins with actin filaments in WRK1 cells: relation to G protein-mediated phospholipase C activation. Proc Natl Acad Sci U S A. 1995; 92(18):8413–8417. [PubMed: 7667304]
53. Riobo NA, Manning DR. Receptors coupled to heterotrimeric G proteins of the G12 family. Trends Pharmacol Sci. 2005; 26(3):146–154. [PubMed: 15749160]
54. Zhao B, Li L, Wang L, Wang CY, Yu J, Guan KL. Cell detachment activates the Hippo pathway via cytoskeleton reorganization to induce anoikis. Genes Dev. 2012; 26(1):54–68. [PubMed: 22215811]
55. Chan EH, Nousiainen M, Chalamalasetty RB, Schafer A, Nigg EA, Sillje HH. The Ste20-like kinase Mst2 activates the human large tumor suppressor kinase Lats1. Oncogene. 2005; 24(12): 2076–2086. [PubMed: 15688006]
56. Marinissen MJ, Tanos T, Bolos M, de Sagarra MR, Coso OA, Cuadrado A. Inhibition of heme oxygenase-1 interferes with the transforming activity of the Kaposi sarcoma herpesvirus-encoded G protein-coupled receptor. J Biol Chem. 2006; 281(16):11332–11346. [PubMed: 16476737]
57. Yu FX, Luo J, Mo JS, Liu G, Kim YC, Meng Z, et al. Mutant Gq/11 Promote Uveal Melanoma Tumorigenesis by Activating YAP. Cancer Cell. 2014; 25(6):822–830. [PubMed: 24882516]
58. Parravicini C, Chandran B, Corbellino M, Berti E, Paulli M, Moore PS, et al. Differential viral protein expression in Kaposi's sarcoma-associated herpesvirus-infected diseases: Kaposi's sarcoma, primary effusion lymphoma, and multicentric Castleman's disease. Am J Pathol. 2000; 156(3):743–749. [PubMed: 10702388]
59. Kaplan LD. Human herpesvirus-8: Kaposi sarcoma, multicentric Castleman disease, and primary effusion lymphoma. Hematology Am Soc Hematol Educ Program. 2013; 2013:103–108. [PubMed: 24319170]
60. Paulsen SJ, Rosenkilde MM, Eugen-Olsen J, Kledal TN. Epstein-Barr virus-encoded BILF1 is a constitutively active G protein-coupled receptor. J Virol. 2005; 79(1):536–546. [PubMed: 15596846]
61. Dupont S, Morsut L, Aragona M, Enzo E, Giulitti S, Cordenonsi M, et al. Role of YAP/TAZ in mechanotransduction. Nature. 2011; 474(7350):179–183. [PubMed: 21654799]
62. Harvey KF, Zhang X, Thomas DM. The Hippo pathway and human cancer. Nat Rev Cancer. 2013; 13(4):246–257. [PubMed: 23467301]
63. Feng X, Degese MS, Iglesias-Bartolome R, Vaque JP, Molinolo AA, Rodrigues M, et al. Hippo-Independent Activation of YAP by the GNAQ Uveal Melanoma Oncogene through a Trio-Regulated Rho GTPase Signaling Circuitry. Cancer Cell. 2014; 25(6):831–845. [PubMed: 24882515]
64. Jenner RG, Boshoff C. The molecular pathology of Kaposi's sarcoma-associated herpesvirus. Biochim Biophys Acta. 2002; 1602(1):1–22. [PubMed: 11960692]
65. Martin D, Galisteo R, Molinolo AA, Wetzker R, Hirsch E, Gutkind JS. PI3Kgamma mediates kaposi's sarcoma-associated herpesvirus vGPCR-induced sarcomagenesis. Cancer Cell. 2011; 19(6):805–813. [PubMed: 21665152]
66. Martin D, Galisteo R, Ji Y, Montaner S, Gutkind JS. An NF-kappaB gene expression signature contributes to Kaposi's sarcoma virus vGPCR-induced direct and paracrine neoplasia. Oncogene. 2008; 27(13):1844–1852. [PubMed: 17934524]
67. Strassburger K, Tiebe M, Pinna F, Breuhahn K, Teleman AA. Insulin/IGF signaling drives cell proliferation in part via Yorkie/YAP. Dev Biol. 2012; 367(2):187–196. [PubMed: 22609549]
68. Leung HJ, Duran EM, Kurtoglu M, Andreansky S, Lampidis TJ, Mesri EA. Activation of the unfolded protein response by 2-deoxy-D-glucose inhibits Kaposi's sarcoma-associated herpesvirus

replication and gene expression. Antimicrob Agents Chemother. 2012; 56(11):5794–5803. [PubMed: 22926574]

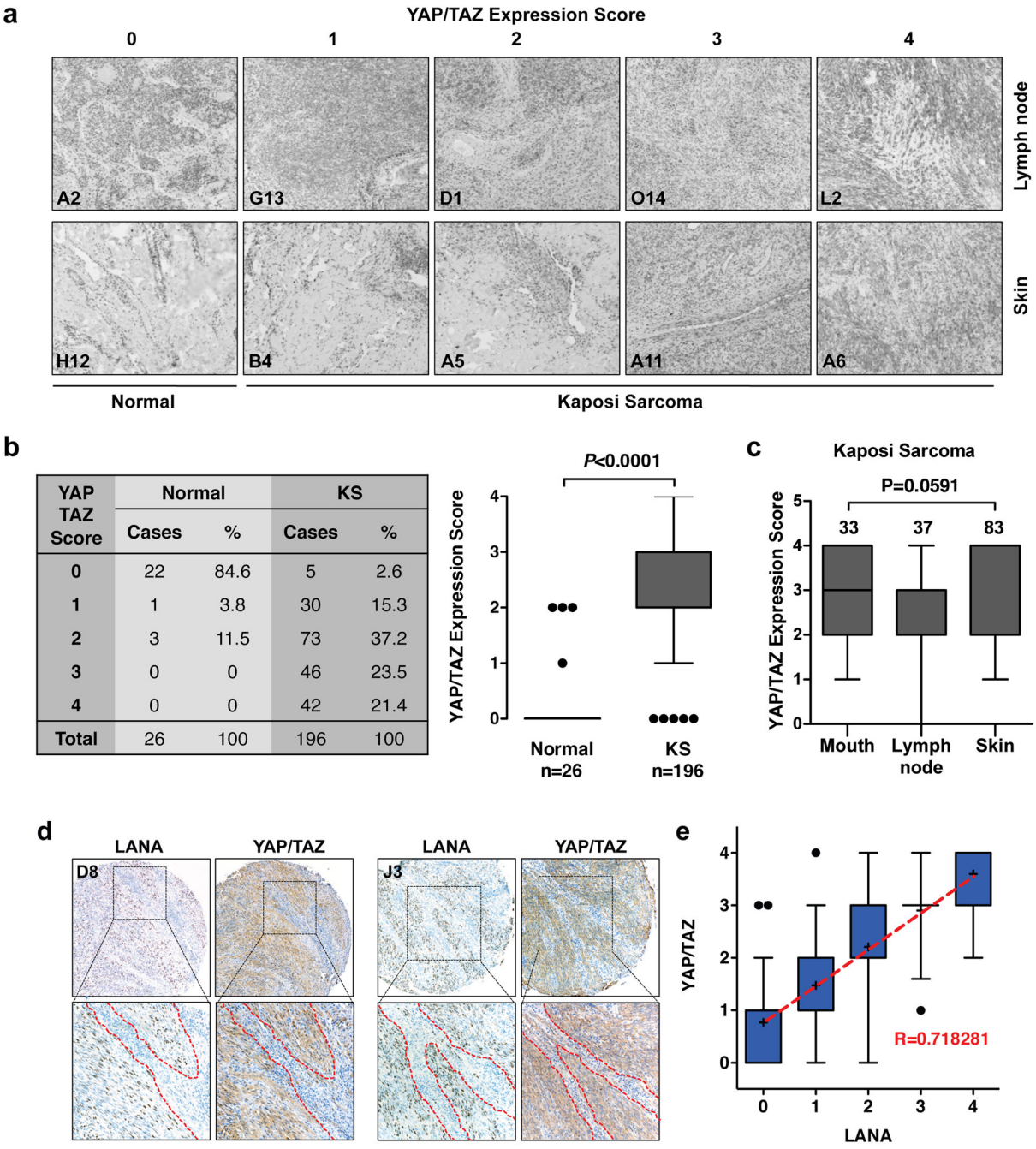

YAP TAZ Score	Normal		KS	
	Cases	%	Cases	%
0	22	84.6	5	2.6
1	1	3.8	30	15.3
2	3	11.5	73	37.2
3	0	0	46	23.5
4	0	0	42	21.4
Total	26	100	196	100

Figure 1.

YAP/TAZ is activated by KSHV in human KS patient tissues. (a) The expression of YAP/TAZ in normal and KS tissues. 222 tissue microarrays were stained with a YAP/TAZ specific antibody. YAP/TAZ expression was scored from 0 to 4 (scores indicated on the top panel) depending on the signal strength of the antibody staining (brown color). Representative YAP/TAZ staining of lymph node and skin from each score are shown. The tissue microarrays sample ID is indicated at lower left corner on each image. (b) YAP/TAZ protein levels are elevated in KS tumors. YAP/TAZ expression was scored from 0 to 4.

Statistical analyses of YAP/TAZ expression score between normal and KS samples are performed. (c) No significant difference is seen in YAP/TAZ expression across different KS lesion sites. KS tissues that have more than ten specimens were statistical and analyzed. (d) YAP/TAZ proteins are co-localized with KSHV in tumor sections. KS tumors were stained with LANA and YAP/TAZ antibodies. Representative tumor sections (with sample ID indicated on the upper left corner) are shown. (e) KSHV expression correlates highly with YAP/TAZ expression. LANA and YAP/TAZ expression was scored from 0 to 4 and recorded for correlation analysis.

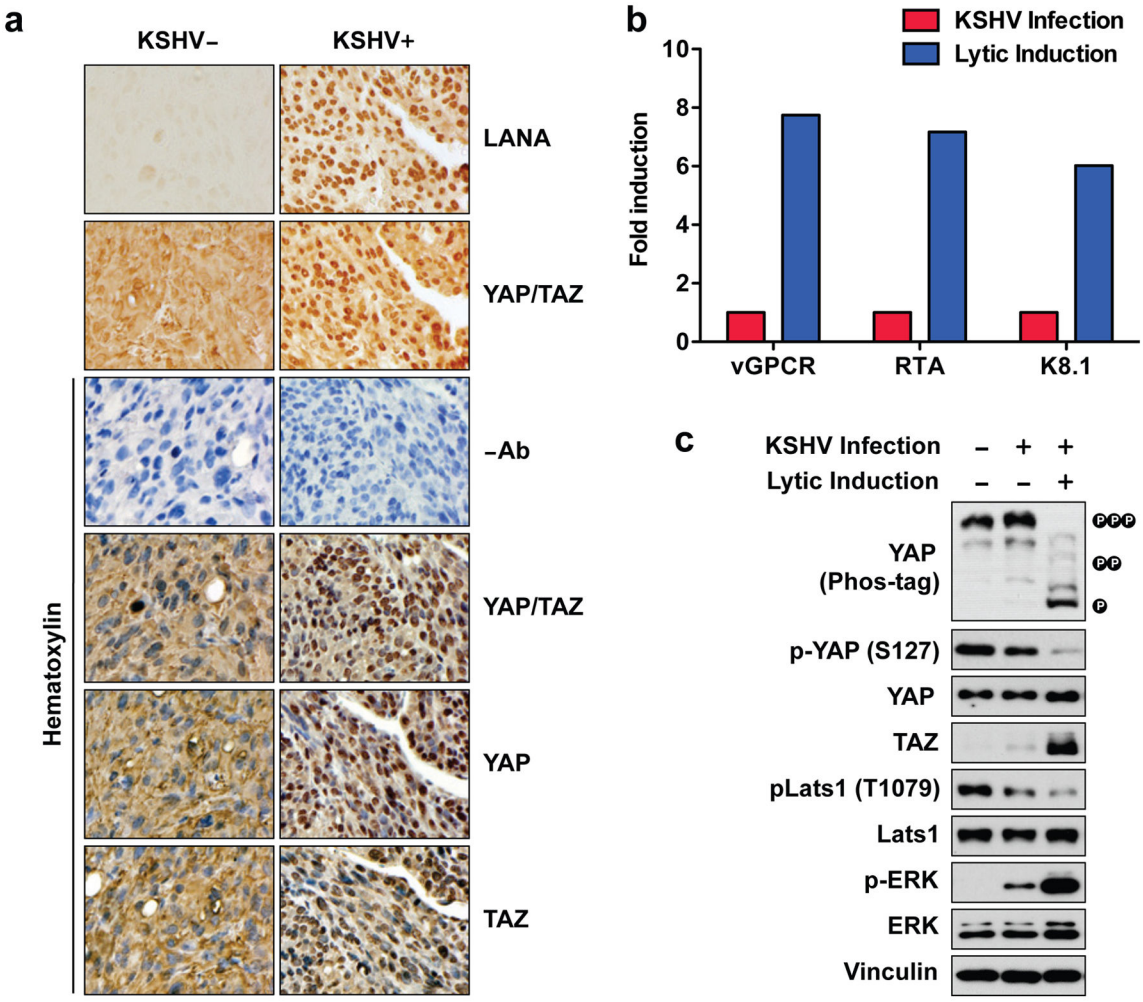

Figure 2.

KSHV stimulates YAP/TAZ activity. (a) IHC staining of YAP/TAZ, YAP, TAZ, or LANA in KSHV-negative or KSHV-positive tumors generated from mECK36 cells. (b) Expression of lytic genes (vGPCR, RTA, K8.1) in adherent HEK293 cells (HEK293A) transfected with recombinant KSHV. Expression of lytic genes was induced by treating cells with 3 mM sodium butyrate for 48 hrs. (c) Expression of lytic KSHV genes induces YAP/TAZ activity. Protein lysates from serum starved adherent HEK293 cells infected with or without KSHV were prepared and subjected to immunoblotting.

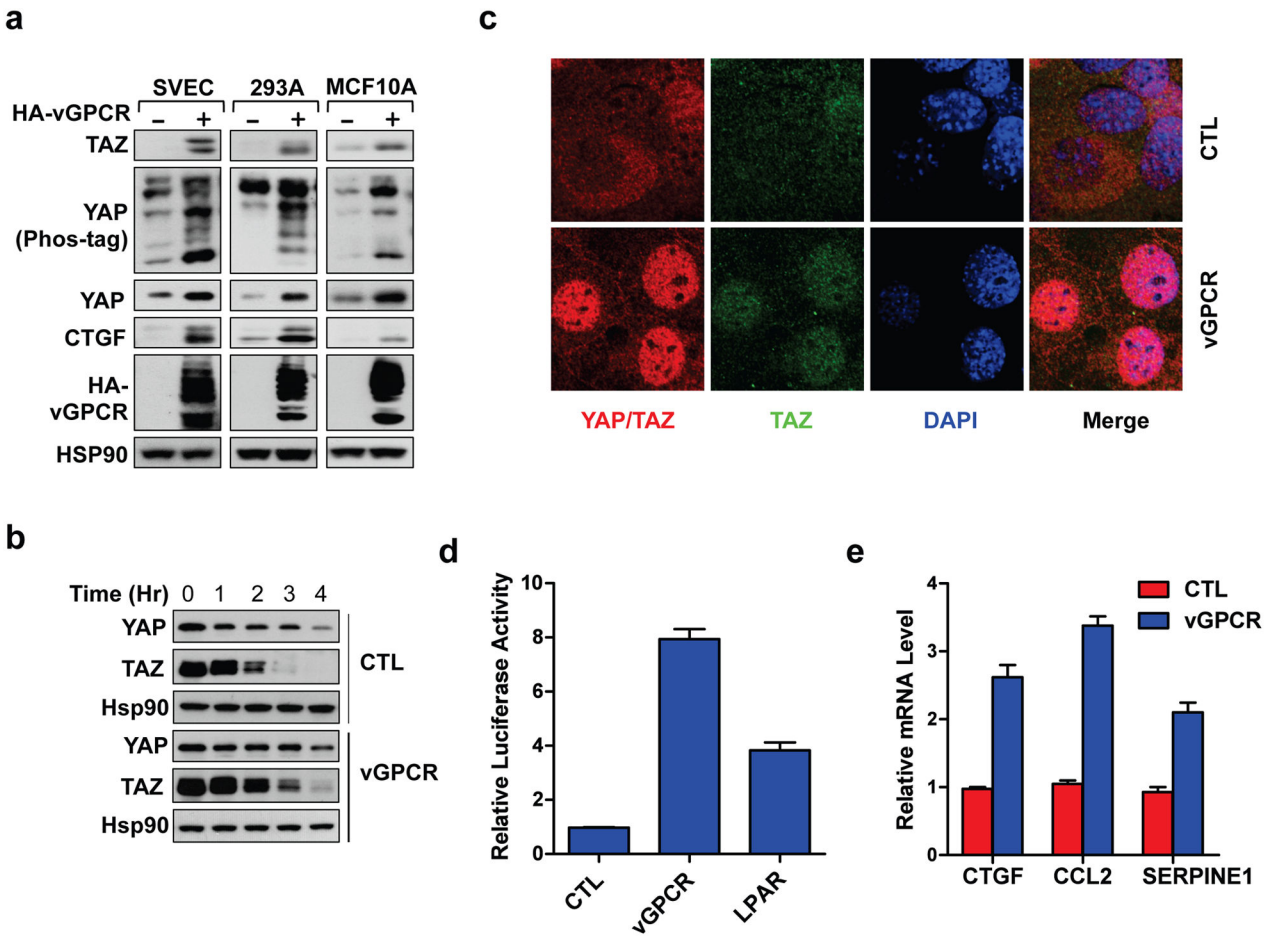

Figure 3.

vGPCR activates YAP/TAZ. (a) vGPCR expression increases YAP and TAZ protein levels. MCF10A, HEK293A, and SVEC cells stably expressing either the vector control or HA-vGPCR were serum-starved for 12 hours before immunoblotting analysis. (b) vGPCR stabilizes YAP/TAZ. HEK293A cells stably expressing vGPCR were treated with cycloheximide for the indicated time (hours: hr). (c) vGPCR induces YAP/TAZ nuclear localization. HEK293A cells overexpressing either control (CTL) or vGPCR were serum-starved for 12 hours. YAP/TAZ subcellular localization were determined by immunofluorescence staining for YAP/TAZ (red), TAZ (green), along with DAPI for DNA (blue). (d) vGPCR activates a YAP/TAZ reporter. Control (CTL), vGPCR, or positive control LPAR plasmids were co-transfected with a 5 X UAS-luciferase reporter, Renilla and Gal4-TEAD4 into HEK293A cell. 24 hours after transfection, cells were serum starved for 12 hours and luciferase activity was measured and quantified by normalization to the co-transfected Renilla. (e) vGPCR induces expression of YAP/TAZ target genes. mRNA levels of indicated YAP/TAZ target genes was measured in stably expressing control (CTL) and vGPCR cells following 12 hour starvation.

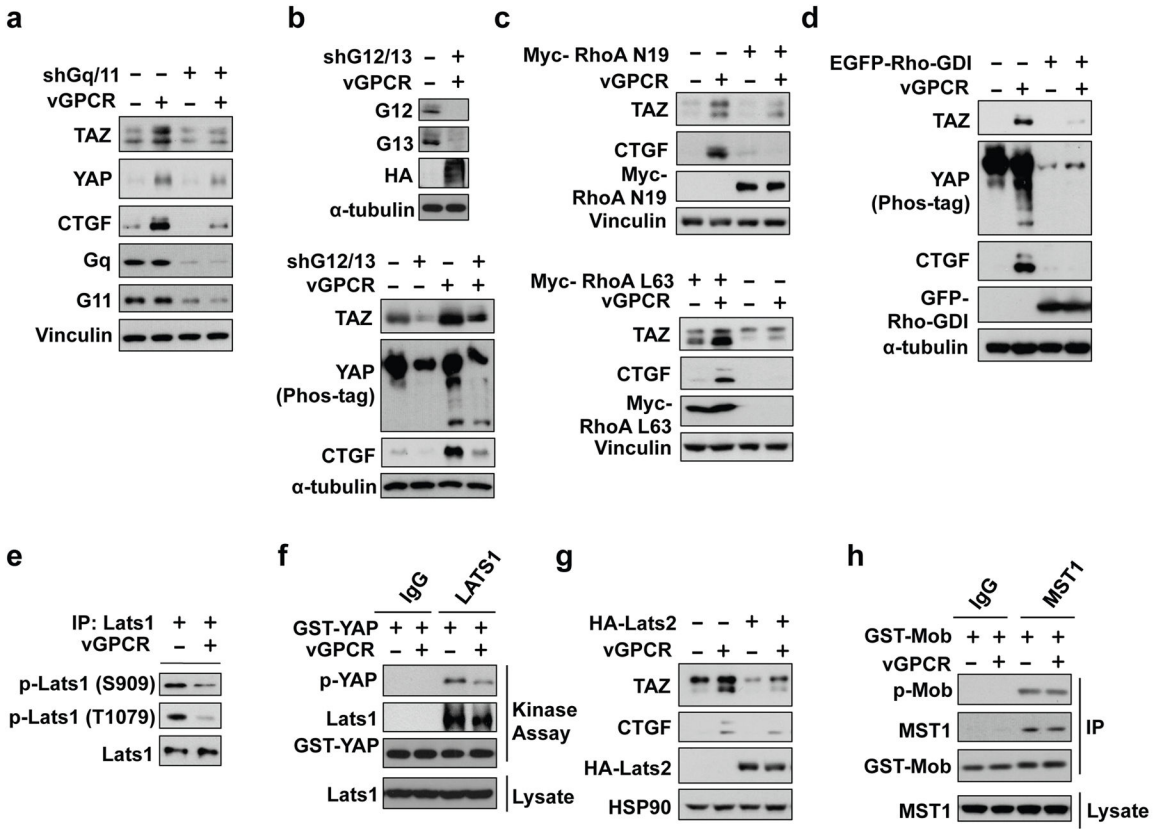

Figure 4.

Mechanism of YAP/TAZ activation by vGPCR. (a, b) Knockdown of Gq/11 or G12/13 suppresses YAP/TAZ activation by vGPCR. shRNAs were used to stably knockdown Gq/11 or G12/13 in the control or vGPCR expressing HEK293A cells. (c, d, g) HEK293A stable control and vGPCR expressing cells were transfected with the indicated plasmids. (e) vGPCR decreases Lats1 phosphorylation. Endogenous Lats1 was immunoprecipitated from control and vGPCR-expressing cells. Lats1 phosphorylation on the activation loop (S909) and hydrophobic motif (T1079) were detected by phosphor antibodies as indicated. (f) vGPCR expression inhibits Lats kinase activity. Lats1 was immunoprecipitated with a control IgG or Lats1 specific antibody as indicated. Kinase activity was determined in vitro using GST-YAP as a substrate. Phosphorylation of GST-YAP was detected by phosphor-specific antibody. (g) Overexpression of Lats2 suppresses the effect of vGPCR on TAZ protein accumulation and CTGF expression. (h) vGPCR does not affect MST1 activity. MST1 was immunoprecipitated from control or vGPCR expressing cells. In vitro kinase activity was measured using GST-Mob as a substrate.

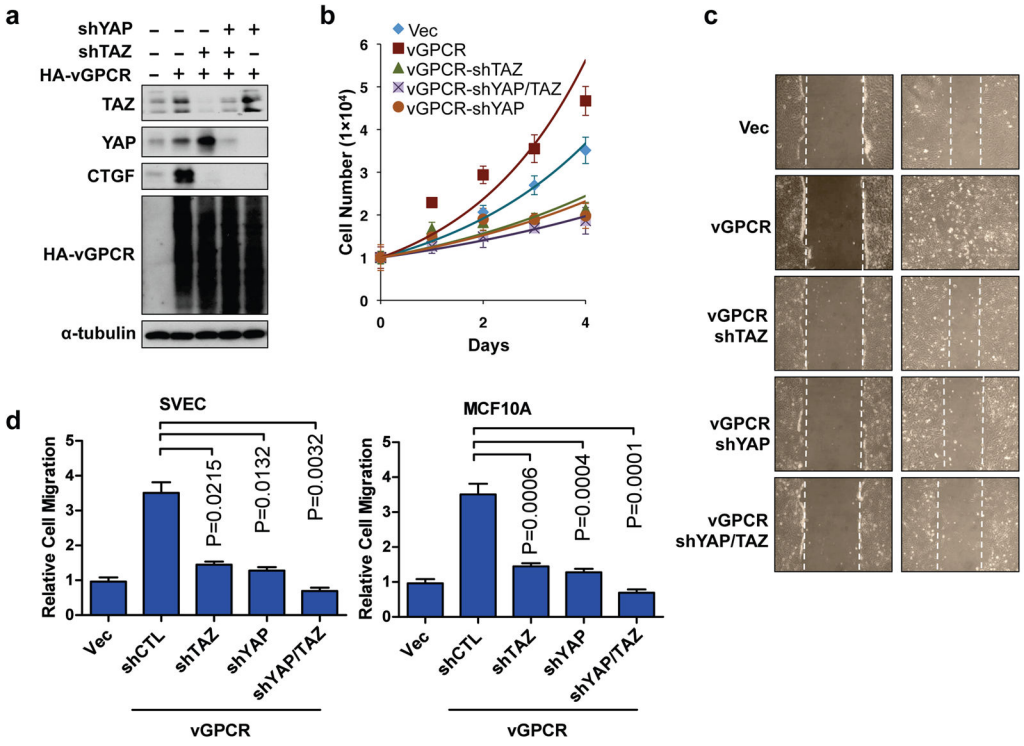

Figure 5.

YAP/TAZ are required to mediate vGPCR-induced cell proliferation and migration. (a) shRNA was used to stably knockdown YAP, TAZ, or YAP/TAZ as indicated in SVEC cells. The knockdown efficiency was confirmed by Western blotting. (b) Knockdown of YAP/TAZ suppresses cell proliferation. SVEC stable cells were seeded (1 X 10^4 cells/well) in medium containing 0.5% serum and counted every 24 hours. (c) YAP/TAZ knockdown inhibits cell migration. A wound healing assay was performed with the indicated SVEC cells. After the scratch, cells were cultured in 0.5% serum containing medium for 16 hours. (d) YAP/TAZ are required for vGPCR induced cell migration. A transwell cell migration assay was conducted in SVEC (upper panel) and MCF10A (bottom panel) cells.

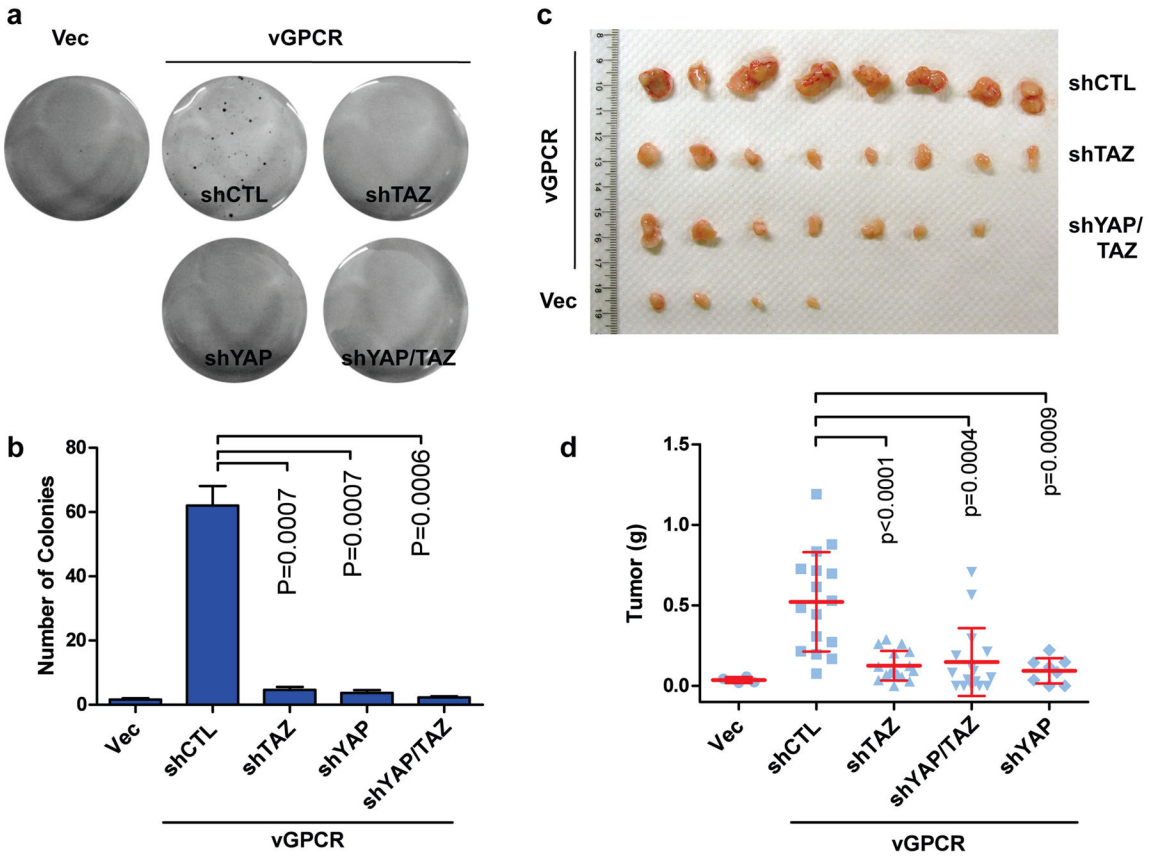

Figure 6.

YAP/TAZ activation is important for vGPCR-induced tumorigenesis. (a, b) YAP/TAZ are essential for vGPCR-induced anchorage independent growth. The stable SVEC cells described in Figure 5a were tested for anchorage independent growth. Cells were seeded at 3 X 10^4 cells/well in 0.4% soft agar medium with hygromycin and puromycin. After twenty days, colonies were visualized with crystal violet staining and quantified. (c, d) YAP/TAZ are important for vGPCR-induced tumorigenesis. 1×10^6 SVEC cells were injected subcutaneously into the flanks of nude mice. Tumors were harvested 5 weeks after injection and weighed.

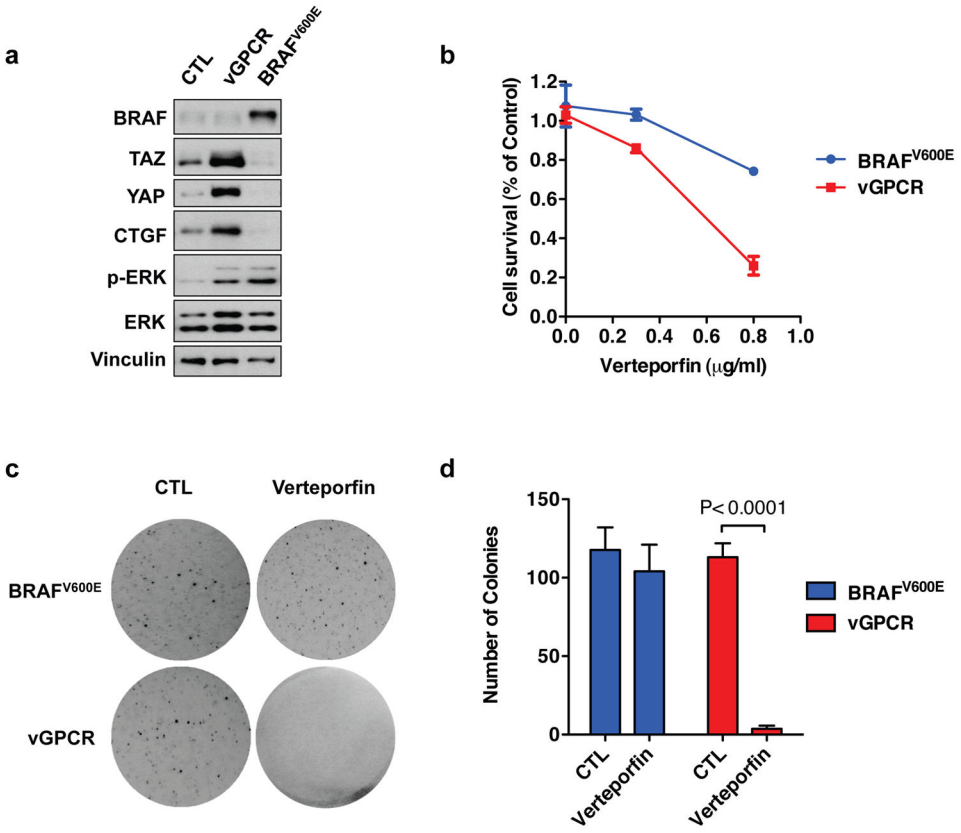

Figure 7.

Sensitivity of vGPCR-expressing cells to YAP inhibition. (a) Stable SVEC cells expressing vGPCR or $BRAF^{V600E}$ were established, and YAP/TAZ protein levels were assessed. (b) Verteporfin inhibits survival of cells expressing vGPCR. SVEC cells expressing vGPCR or $BRAF^{V600E}$ were seeded at same density, and treated with different doses of verteporfin for 72 hrs, cell numbers are then counted. (c, d) Verteporfin inhibits anchorage-dependent growth of cells expressing vGPCR. SVEC cells expressing vGPCR or $BRAF^{V600E}$ were seeded into soft agar at 3 X 10^4 cells/well. selected groups of cells were treated with 0.3 μM Verteporfin. After twenty days, colonies were visualized with crystal violet staining and quantified.